

Gellation of rigid filament networks

B.A. DiDonna

Department of Chemistry and Biochemistry, University of California Los Angeles, Los Angeles, CA 90095, USA

D.C. Morse

*Department of Chemical Engineering and Material Science,
University of Minnesota, Minneapolis, MN 55455-0436, USA*

(Dated: August 14, 2018)

We consider a model for gelation of rigid rods, in which rods that are initially placed at random undergo diffusion, and form cross-links when they collide. In the limit of point-like cross-links, the number N of crosslinks per rod approaches $N \simeq 3.53$. In a model with compliant cross-links of maximum length ℓ_c , $N(t)$ increases with time as $N(t) \propto \text{const.} + cL^2\ell_c \ln(t)$, where c is concentration and L is rod length.

PACS numbers: 61.46.Df, 82.70.Kj, 87.15.Aa

I. INTRODUCTION

The basic physics of networks of rigid and semiflexible filaments has proved to be important to many systems of current interest. Carbon nanotubes in a buffered solution have very strong localized interactions which can be modeled as permanent cross-links¹. Similarly, microtubules and actin filaments in the cytoskeleton have long persistence lengths and are cross-linked by a number of chemical agents². Still, there is very little knowledge concerning the generic properties of cross-linked gels created from long, thin filaments with high bending rigidity. There is not even a consensus on the expected connectivity of such gels. Without some understanding of connectivity, it is impossible to formulate *ab initio* models for the electrical and thermal conductivity of these systems, much less their rheological properties.

Previous numerical simulations of the gelation of rigid rod networks^{3,4} have taken a purely geometrical constructive approach: In this approach, straight filaments with a nonzero diameter d and a large aspect ratio L/d are placed in a unit cell at random, and are assumed to be attached only if they overlap. In a three dimensional system, the number of cross-links formed in this way depends directly upon the rod diameter, and vanishes in the limit of infinitely thin chains. The situation is, of course, very different in a two dimensional model, for which this approach can yield a percolation threshold for infinitely thin rods. There is also a rich literature on both connectivity and rigidity percolation in networks of rods^{5,6,7,8,9}, which rely on such static, constructive approaches to building a network. However, when three dimensional networks are created in this way, they contain many near misses, which would be transformed into cross-links if the rods were allowed any mobility. The number of close approaches just outside the overlap cut-off scales with the density of the system. Thus, as we will show, this approach vastly underestimates the maximal number of connections that can be formed in a three dimensional system if the rods are allowed to diffuse.

Here, we consider a simple dynamical model in which

gelation instead occurs as the result of Brownian motion of thin rods. Rods are initially placed at random and then undergo Brownian motion. Pairs of rods are assumed to irreversibly form cross-links whenever the distance of closest approach falls below some “capture radius”. Throughout this paper, we consider only “flexible” cross-links that exert no torque, which thus do not introduce a constraint or bias on the angle between cross-linked pairs of rods. The simplest variant of such a model is one in which rods cross-link when they collide, and form a permanent point-like (but rotationally flexible) cross-link at the point of collision. In this limit, the cross-linking would proceed to a well defined saturation point: The creation of cross-links would continue until the system was mechanically rigid, i.e., until the constraints imposed by the cross-links allowed no further motion of the network.

We may estimate a lower bound on the number of cross-links created in this idealized limit of point-like cross-links by simple degree of freedom counting: Each rod has 5 rigid motion degrees of freedom (three translations and two physically relevant rotations, excluding axial rotation). Each cross-link introduces three constraints, or removes 3 degrees of freedom, by equating the positions of the points along two rods at which those rods collide. This argument thus predicts that the total ratio of cross-linkers to rods at the rigidity transition should be $5/3$. Since each cross-link connects two rods, the average number of rods to which a randomly chosen rod is connected is predicted to be $10/3 = 3.333$.

This estimate is expected to underestimate the number of cross-links somewhat, because it assumes that the constraints introduced by random cross-links are all linearly independent. It is possible for the system to form cross-links that are, in a sense, redundant. The simplest example of this occurs when a rod that is cross-linked at two points to a network that would remain rigid if this rod was removed. The two cross-links required to immobilize this rod introduce 6 constraints into the system of equations required to describe the system, but remove only the 5 degrees of freedom associated with that rod,

thus “wasting” one constraint. As a result of this kind of redundancy, one might expect the average number of attachment points per rod to be slightly higher than $10/3$ (as is found to be the case).

The idealized limit of point-like cross-links discussed above is, however, very difficult to directly simulate, as well as being physically unrealistic for many systems of interest. The most straightforward way to simulate the Brownian motion of a partially gelled system of rods with point-like cross-links would be to introduce Lagrange multiplier forces for each of the cross-links. A Brownian dynamics simulation of the system with such cross-links would then require the solution of a large system of linear equations every time step in order to determine the constraint forces exerted by the cross-links. This would be prohibitively expensive for all but very small systems or short simulations.

Here, we instead consider a system of slightly compliant cross-links, in which the distance between the cross-link attachment points on a pair of rods is constrained to remain less than some maximum cross-link length ℓ_c . A network with compliant cross-links retains some flexibility even when the number of cross-links would arrest all motion in a corresponding network of point-like cross-links. As a result, the number of cross-links in such a system never truly saturates, but increases more and more slowly, as the addition of further cross-links requires more and more rare thermal fluctuations. We find that this creates a very slow logarithmic growth in the number of cross-links with time at late times. We show, however, that it is possible to extract information about the number of cross-links that would be formed in the idealized limit of point-like cross-links by running simulations with several values of ℓ_c and extrapolating the results to $\ell_c = 0$.

II. SIMULATION

Our simulated systems consist of rigid filaments modeled by straight line segments of unit length $L = 1$. The initial state of the system is prepared by placing the rods in a simulation box with uniformly distributed random positions and orientations. We simulated dimensionless rod number concentrations $\bar{c} \equiv cL^3$ in the range $2 < \bar{c} < 2000$. Each system is run with at least 1000 filaments and a box volume $\geq 10L^3$. Periodic boundary conditions are enforced. The filaments are moved one at a time in random order via an unconstrained Brownian dynamics algorithm. For each filament the transverse, longitudinal, and rotational displacements were calculated separately, with drag coefficients chosen so that the transverse and rotation diffusion constants were respectively

$$D_{\perp} = \frac{1}{2}D_{\parallel}$$

$$D_r = 6D_{\parallel}/L^2,$$

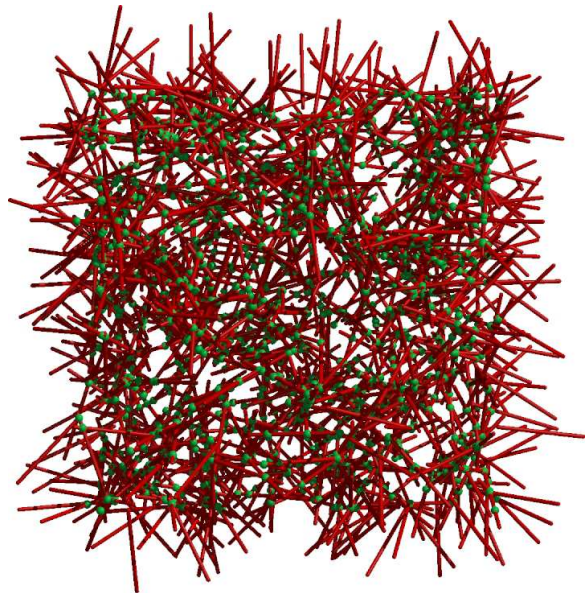


FIG. 1: Random distribution of 1000 rigid filaments with density $\bar{c} = 10$. For filaments which cross the boundaries, both periodic images are shown. The diameter of the filaments are 0.0052 times their length.

where D_{\parallel} is the longitudinal diffusion constant¹⁰.

In the simulations presented here, a permanent cross-link is created between two filaments whenever a Brownian dynamics move would have caused one of the filaments to cut through the other. Though not presented here, we found quantitatively similar results when the cross-linking criterion was that two filaments approached within a finite capture radius of one another. The cross-link connects the two rods at their points of intersection. To inhibit bundling, only one cross-link was allowed between any two filaments. For dense systems and rigid filaments, bundling proved not to be an issue, since trapped entanglements did not allow filament alignment.

The constraints of cross-link compliance and topology conservation are enforced via a Monte-Carlo acceptance criterion, as in Ref.¹¹ – motions which cause the center-lines of neighboring filament to cross or which cause the length of any existing cross-link to exceed a maximum value are rejected. In some cases we also enforce a hard core potential between rods using the same technique. Unless otherwise stated, our simulated filaments have zero excluded volume. Cross-links imposed no rotational constraints about their axes.

As we show in the next section, we can easily extrapolate from our data to the case of zero radius cross-links $\ell_c = 0$. We note, however, that direct simulation of cross-links that are completely noncompliant to stretching is impracticable via any simulation technique. We also comment that we are pursuing similar simulations using molecular dynamics on bead-chain polymers, but such systems are unable to approach the limit of infinite bend rigidity.

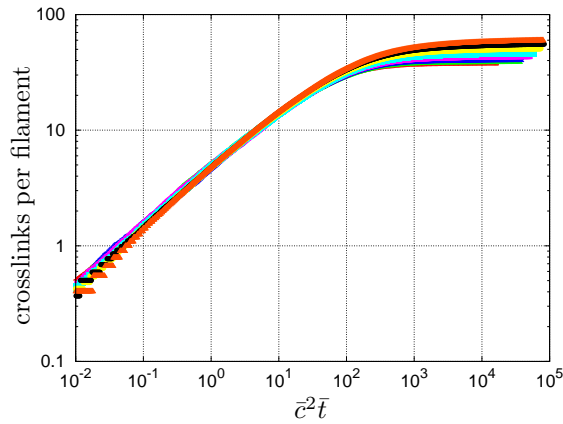


FIG. 2: Time evolution of cross-linking number for $\bar{\ell}_c = 0.0013$ and, from lowest to highest curves respectively, $\bar{c} = 100, 150, 200, 300, 400, 600, 800$, and 1000 . The early time evolution of all the plots collapsed when plotted versus $\bar{c}^2 \bar{t}$, where time is measured in units of the rotational diffusion time $1/6D_r$.

III. RESULTS

A. Cross-link number

Immediately after cross-linking was initiated the number of cross-links was found to grow as $\bar{c}\sqrt{\bar{t}}$ (see Figure 2), where dimensionless time \bar{t} is measured in units of the rotational diffusion time $1/6D_r$. This power law growth ends at a crossover time of order $\bar{t} \sim 100/\bar{c}^2$. We associate this crossover time with the time necessary for a filament to sense its neighbors by diffusion, since the distance to nearest neighbors (corresponding to the "cage diameter" in the Doi model of entangled rigid rods) is proportional to $1/\bar{c}$. The power law growth was followed by a period of slow logarithmic growth. The prefactor of the logarithm was observed to increase for larger dimensionless cross-link radius $\bar{\ell}_c \equiv \ell_c/L$ or higher concentration \bar{c} . We simulated many combinations of these parameters in the range $0.0013 \leq \bar{\ell}_c \leq 0.013$ and $5 \leq \bar{c} \leq 2000$. All simulations were run with dimensionless time-steps 10^{-9} , because we found that the time dependent evolution had nearly converged for time-steps on this order of magnitude. Obtaining a half decade of logarithmic growth on a system of 1000 or more filaments typically took 12 days on a single 3.2 GHz Xeon based Linux system. Each data point presented here represents the average of four independent systems.

Figure 3 shows our numerical fits to the scaling data. We fit the late time scaling in cross-link number for each concentration to the form $A \log(\bar{c}^2 \bar{t}) + B$ via parameters A and B . Independent fits of A and B to powers of \bar{c} and $\bar{\ell}_c$ indicated that the overall scaling was consistent with a pure dependence on the dimensionless combination $\bar{c}\bar{\ell}_c$. This simple dependence seemed more physically plausible, so we restricted our fits to this combination. We

fit the value of A to a form $\alpha \bar{c}\bar{\ell}_c$ via parameter α and the coefficient B to a form $\beta + \beta' \bar{c}\bar{\ell}_c$ via the parameters β and β' . The parameter β' may be absorbed into the logarithm as a multiplicative constant $\gamma = \exp(\beta'/\alpha)$.

The result of this fitting procedure was the following form for the cross-link number:

$$\begin{aligned} N &= \beta + \alpha \bar{c}\bar{\ell}_c \log(\gamma \bar{c}^2 \bar{t}) \\ \alpha &= 0.0846 \pm 0.0013 \\ \beta &= 3.53 \pm 0.033 \\ \gamma &= 4.51 \times 10^6 \pm 2.2 \times 10^5 \end{aligned} \quad (1)$$

We chose to restrict our linear fit of the parameter B to the region $\bar{c}\bar{\ell}_c \leq 1.5$, which seemed to converge linearly to the value $B = 3.53$ for asymptotically small $\bar{c}\bar{\ell}_c$. Higher values measured for $\bar{c} = 200$ and $0.078 \leq \bar{\ell}_c \leq 0.013$ deviated significantly from this linear fit. This deviation may result from three body interactions for very large values of cross-link radius $\bar{\ell}_c$, or it may simply result from our time-step being too large under these very extreme conditions. Unfortunately, since these simulations were run at the limit of our current computational capability, clarification will have to wait for future work. Though data is not included here, the cross-link number was seen to deviate upward from the fitted linear relation for $\bar{c} \leq 10$ – we will discuss this discrepancy further below.

In the next section we develop arguments, based on additional measurements, for the physical origin of each term in Eq. 1. We link the constant term to the rigidification threshold linking number for unstretchable cross-links and the term linear in \bar{c} and $\bar{\ell}_c$ to localized motion within the cross-link length. We attribute the logarithmic growth term to collective motion of the system. The logarithm reflects slow, glassy dynamics.

B. Cross-link statistics

To shed light on the origins of the cross-linking number in Eq 1, we examine another informative statistic: the radial distribution function of unbound neighbors to a given rod. It can be shown¹² that for a random spatial distribution of non-interacting rods, given a test rod, the probability that another rod will have a distance of closest approach between a radius r and $r + dr$ is given by

$$P(r)dr = \frac{\pi}{2} c L^2 dr. \quad (2)$$

Thus, without cross-linking, the probability of finding a neighboring rod with closest approach at any given radius is independent of the radius.

Figure 4 shows the measured distribution for the distance of closest approach of unlinked neighbor filaments to a given test filament, averaged over all filaments. The

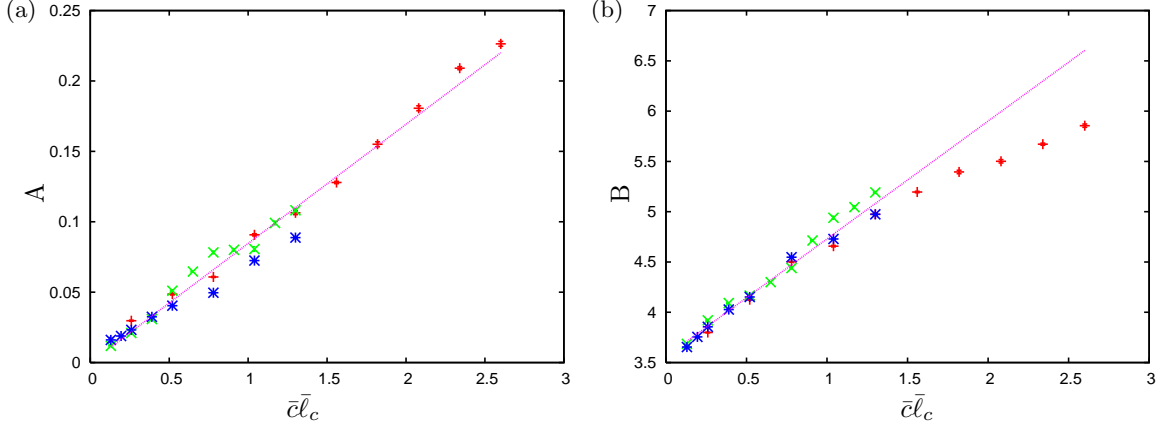


FIG. 3: Fitting parameters A and B from a fit to the form $A \log(\bar{c}^2 t) + B$ for the late time evolution of cross-link number, plotted as a function of the product $\bar{c} \bar{\ell}_c$. Crosses are for runs with constant $\bar{\ell}_c = 0.0013$, stars are for runs with constant $\bar{c} = 100$, and plus symbols are for runs with constant $\bar{c} = 200$. Straight lines are linear fits of A to $\alpha \bar{c} \bar{\ell}_c$ and B to $\beta + \beta' \bar{c} \bar{\ell}_c$.

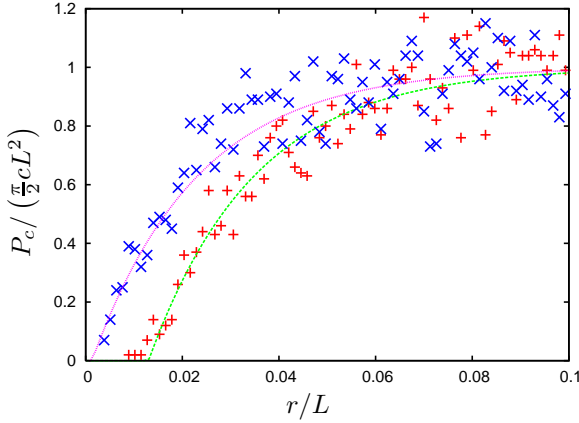


FIG. 4: Radial distribution function for distance of closest approach of unlinked neighbor filaments. All data is for a concentration of $cL^3 = 100$. The upper and lower data sets are respectively for $\ell_c/L = 0.0013$ and $\ell_c/L = 0.013$. Solid lines are the predicted distribution from Eq 3 with $b = 1$.

measured probability function is well fit by the function

$$P_c(r) \approx \begin{cases} 0 & r \leq b\ell_c \\ \frac{\pi}{2} c L^2 \left(1 - \exp\left(-\frac{\pi c L^2}{2 \times 3.53} (r - b\ell_c)\right) \right) & r > b\ell_c \end{cases} \quad (3)$$

where the value of b grows with time. At any given time, when $P(r) - P_c(r)$ is integrated from zero to infinity it gives exactly Eq. 1 for the number of cross-links which each filament has captured on average. More specifically, the constant term in Eq. 1 comes from integrating the exponential term in Eq 3, and all the other terms in Eq. 1 comes from integrating the depleted region between $0 < r < b\ell_c$ in Eq 3.

We interpret Eq 3 as proof that the extrapolated linkage number $N = 3.53$ is exactly the linkage number required for rigidification of line segments in 3-dimensional

space, which we shall call N_r . If the cross-links had no stretching compliance ($\ell_c = 0$), then after N_r cross-links per filament had been added the lattice would become completely elastically rigid. In this case, there would be no further spatial fluctuations, and the cross-linking would cease. Prior to the rigidity transition, the filaments should diffusively explore their local environment up to the point when they have encountered and linked to N_r other rods on average. Since the probability of finding a rod at any given radius is a flat distribution, the probability of finding N_r rods *within* radius r is exponential, with form

$$\exp\left(-\frac{\pi c L^2}{2 N_r} r\right).$$

This form correspond exactly to the exponential in Eq 3 if we make the identity $N_r = 3.53$. This measured value is close to the theoretical lower bound of $N_r = 10/3$ which we derived in the introduction.

We note that as \bar{c} approaches the value $\frac{2}{\pi} \times 3.53 \sim 2.2$, the decay length in Eq. 3 approaches L , so that rod end effects will become more important. In this limit the rods will interact more like point-like particles. This is consistent with our observation (not shown) of a deviation upward from the logarithmic fit in Eq. 1 for $\bar{c} \leq 10$.

The effect of finite cross-link length is less straightforward to interpret. After the rigidity connectivity N_r has been reached the only possible fluctuation motion of any filament is within the stretch compliance of cross-links to its neighbors. The density of neighbors within the cross-link length is higher than outside, and without collective motion of its neighbors, there is very little room for a filament to move around in. Our results suggest that filaments quickly explore a region of radius r_c , producing the linear term in Eq 1. At long times, they continue to sample and link to neighbors in the space around them, increasing their sampling radius at a logarithmic rate. Furthermore, the exponential in Eq 2 is shifted by this

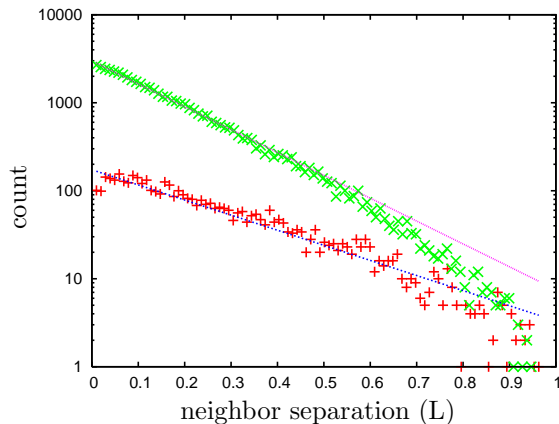


FIG. 5: Distribution of cross-link separation lengths for late time systems with $\bar{\ell}_c = 0.0013$ and $\bar{c} = 150$ (lower curve) or $\bar{c} = 1000$ (upper curve). Straight lines are theoretically predicted exponential curve for random cross-link placement, disregarding end effects.

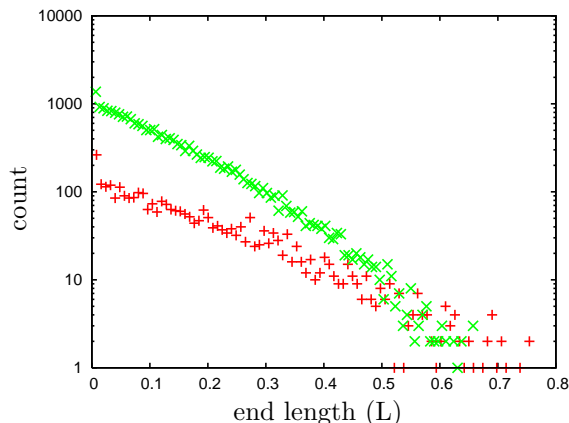


FIG. 6: Distribution of lengths between filament ends and nearest cross-link for late time systems with $\bar{\ell}_c = 0.0013$ and $\bar{c} = 150$ (lower curve) or $\bar{c} = 1000$ (upper curve).

sampling radius, so that $P_c(r)$ goes smoothly to zero at the edge of the depletion zone. This is consistent with the slow, glassy dynamics of large scale collective motions in the presence of deep potential wells.

Finally, we analyze the statistics of cross-linking. In Figure 5, we plot the distribution of separations between neighboring cross-links. As expected, the distribution is exponential, with decay constant equal to the average density of cross-links per unit length. The exponential

decay is modified slightly by finite filament length effects at separations approaching L . In Figure 6, we plot the distribution of lengths of “dangling” ends beyond the last cross-link on each filament, which is also exponential. These observed distributions are consistent with spatially random placements of cross-links along the filament, and are qualitatively the same as for flexible polymers.¹³

IV. DISCUSSION

We have found a new generic number for the maximum cross-linking in the limit of vanishing cross-link length, $N_r = 3.53$. We further speculate that this is the as yet undiscovered rigidification threshold coordination number for a random lattice of rigid, line-like filaments in 3 dimensions. We have also found that the cross-link number depends logarithmically on time and linearly on both cross-link length and filament concentration, and we have measured the linear coefficient.

It is worth comparing our results to percolation based Monte-Carlo studies without particle dynamics. Foygel et al.⁴ found that the percolation threshold for randomly distributed but stationary rods with aspect ratio a occurred at number density $\bar{c} \approx 0.76a$ with an average cross-linking number $N = 1.2$. Comparing their simulations to ours, their aspect ratio is equivalent to $1/(2\bar{\ell}_c)$. Thus for $\bar{\ell}_c = 0.0013$, a typical value in our simulations, *connectivity* percolation would not occur below $\bar{c} \approx 290$, and even at this value filaments would have around 1.2 overlaps on average. Thus, the addition of dynamics and localized bonding between filaments dramatically increases the connectivity of the filament suspension.

An future extension to this work will be the addition of a finite filament bend modulus. For large bend modulus, we expect the transverse filament fluctuations will be equivalent to an increase in capture radius. This research is under way. It would also be interesting to study the effect of the initial configuration on the cross-link number – initial alignment of the filaments might greatly increase the tendency towards bundling, thereby increasing the cross-link number significantly.

Acknowledgments

BD thanks Gary Grest and Pieter In't Velt for enlightening discussions. BD acknowledges partial support from the Institute for Mathematics and its Applications with funds provided by the National Science Foundation.

¹ L. A. Hough, M. F. Islam, B. Hammouda, A. G. Yodh, P. A. Heiney, *Nano Letters* **6** 313 (2006).

² B. Alberts, D. Bray, J. Lewis, M. Raff, K. Roberts, and J.D. Watson, *Molecular Biology of the Cell*, 3rd edition (Garland, New York, 1994).

³ I. Balberg, N. Binenbaum, and N. Wagner, *Phys. Rev. Lett.* **52**, 1465 (1984).

⁴ M. Foygel, R. D. Morris, D. Anez, S. French, and V. L. Sobolev, *Phys. Rev. B* **71**, 104201 (2005).

⁵ D. A. Head, A. J. Levine, and F. C. MacKintosh, *Phys.*

- Rev. Lett.* **91**, 108102 (2003).
- ⁶ J. Wilhelm and E. Frey, *Phys. Rev. Lett.* **91**, 108103 (2003).
 - ⁷ M. Sahaimi and S. Arbabi, *Phys. Rev. B* **47**, 695 (1993),
M. Sahaimi and S. Arbabi, *Phys. Rev. B* **47**, 703 (1993).
 - ⁸ C. Moukarzel and P. M. Duxbury, *Phys. Rev. E* **59**, 2614 (1999).
 - ⁹ D. J. Jacobs and B. Hendrickson, *J. Computational Physics* **137** 346 (1997).
 - ¹⁰ M. Doi and S. F. Edwards, "The Theory of Polymer Dynamics" Oxford University Press, New York (1986).
 - ¹¹ Shriram Ramanathan and David C. Morse, *J. Chem. Phys.* **126**, 094906 (2007).
 - ¹² S. Ramanathan, Ph.D. Thesis, University of Minnesota (2006).
 - ¹³ G. S. Grest and K. Kremer, *Macromolecules* **23** 4994 (1990).